ACS APPLIED MATERIALS & INTERFACES

RESEARCH ARTICLE

www.acsami.org

Spectral and Physical Properties of Electrochemically Formed Colored Layers on Titanium Covered with Clearcoats

Andrew Munro,[†,‡] Michael F. Cunningham,[‡] and Gregory Jerkiewicz*[,†]

[†]Department of Chemistry, Queen's University, 90 Bader Lane, Kingston, Ontario K7L 3N6, Canada

[‡]Department of Chemical Engineering, Queen's University, 19 Division Street, Kingston, Ontario K7L 3N6, Canada

ABSTRACT: We present the application and characterization of two commercial polymer clearcoats to electrochemically formed colored passive layers on titanium with the aim of providing physical protection required in many of titanium's applications, while allowing the unique appearance of the colored layers to show through. Thin layers of an acrylic automotive clearcoat (~3.5 μm thick) and an epoxy marine clearcoat (~6.5 μm thick) are applied to the colored titanium surfaces using spin coating, and are found to slightly modify their visual properties, while maintaining their bright, well-defined sparkling colors. Both clearcoats are found to significantly reduce the surface roughness, thereby reducing potential wear from friction and the adhesion of fine dirt particles. They are also found to notably decrease the wetting properties of colored titanium, furthering its protection against damage from ambient and aqueous media. The clearcoats show the ability to protect colored titanium from physical and chemical damage, with the automotive clearcoat exhibiting superior adhesion. Our electrochemical coloring technique combined with the application of clearcoats creates a new and unique system that does not rely solely on a polymer coating for its colorful appearance and protection against corrosion.

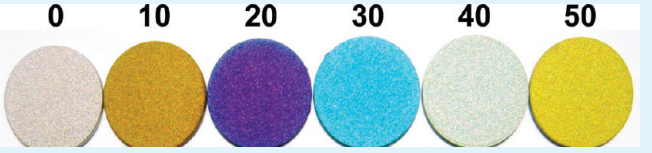

KEYWORDS: materials electrochemistry, titanium, surface characterization, titanium oxides, optical properties

INTRODUCTION

The excellent physical and mechanical properties of titanium (Ti), coupled with its superior corrosion resistance, make it a suitable material for many industries with countless applications. However, Ti is regarded as a poor surface with respect to painting as many commercial paints adhere weakly to it, resulting in chipping and blistering of the coating.[1,2] This is a particular problem in the aerospace industry where chipping and blistering reduce both the appearance and the corrosion resistance initially offered by the paint. As merchandise made of Ti is innumerable (bicycle frames, eyeglass frames, golf clubs, automobile parts, marine vessel fittings and trimmings, aircraft components, jewelry, etc.), the benefits offered by an improved system of protection that simultaneously provides unique esthetics would be profound. It is for this reason that the electrochemical coloring of Ti, which increases its resistance to corrosion while simultaneously offering unique visual properties, is of commercial interest. Electrochemical passivation of Ti is routinely used in the field of biomaterials with the aim of improving the biocompatibility of medical implants made of Ti and its alloys.[3−8] This and other previous approaches focused on the application of direct current (DC) polarization (anodization) to Ti in order to induce the growth of a thick passive layer that would be more stable in various media than Ti alone. Previous results from our laboratory, however, showed that the electrochemical coloring of Ti in aqueous NH_4BF_4 by the application of alternating current (AC) polarization results in bright and uniformly colored passive layers whose thicknesses increase as the applied AC voltage (V_{AC}) is raised.[9−11] There is a linear relationship between the V_{AC} applied to form the colored layers and their thickness, which determines the coloration. The colored layers offer protection against corrosion in mild acidic and basic media as well as in simulated body fluids. As such, this preparation method offers a novel approach to treating biocompatible and dental materials that require enhanced biocorrosion protection and coloration (subcutaneous implants, orthodontic archwires). Those contributions focused on the influence of various experimental parameters on the coloration as well as the thickness, composition, morphology, and corrosion properties of the colored layers.[11]

In certain applications (sporting equipment, sculptures, aircraft components, jewelry, etc.) Ti would benefit not only from an electrochemically colored surface layer, but also from a hard, stable polymer coating. The successful application of a polymer clearcoat that protects the colored layer while allowing the unique coloration to show through would introduce an innovative alternative to conventional painting, creating a system that does not rely solely on the polymer coating for its appearance or protection against corrosion and weathering. Currently, most of the work on coating Ti in such a manner focuses on the application of thin polymer coatings to untreated Ti in order to increase its effectiveness as a biomaterial.[12−14] In this contribution, we report on the application and characterization of two commercial polymer clearcoats to electrochemically colored Ti. The first is an acrylic automotive clearcoat, chosen on the basis

Received: January 6, 2011
Accepted: March 2, 2011
Published: March 16, 2011

that along with being proven effective in many of Ti's commercial application environments, it is also transparent, allowing the unique visual properties of the passive layers to show through. The second is an epoxy marine clearcoat, chosen as it also possesses the above-mentioned qualities, yet exhibits different types of chemical resistance.[15] Spin-coating was the application technique used as it is suitable for small substrates and typically produces smooth, uniform coatings.

Acrylics offer excellent durability and inertness, as well as impressive transparency. They also offer high gloss, toughness, aging stability and durability to the atmosphere.[16] Acrylics are mostly used as product finishes on automobiles, refrigerators, and other industrial and domestic products requiring a durable, long-lasting coating.

Epoxies are popular as protective coatings because of their excellent adhesion and broad chemical resistance. Epoxies create very hard coatings and make for a good machinery finish.[16] They are generally able to adhere to clean metals and offer strong resistance to acids, alkalis and most solvents.

The objectives of this work were the application of clearcoats and the subsequent characterization of the substrate/coating systems with particular attention paid to how the clearcoats influence the visual properties and modify the physical characteristics of the colored layers. The characterization consisted of analyzing the thicknesses of clearcoat layers using surface profilometry, their influence on the visual properties of the colored layers by recording reflectivity spectra in the visible (vis) region of the electromagnetic spectrum, their impact on the surface roughness of colored Ti through surface topography mapping, their effect on the wetting properties of colored Ti by executing static water contact angle measurements, and their adhesion to the colored layers by performing ASTM adhesion standard D3359−02 tests.

EXPERIMENTAL SECTION

Materials. Disc-shaped samples were employed as electrodes and substrates. The Ti discs were made of commercially pure Ti (Johnson-Matthey, 99.7% Ti, 0.1225% O, 0.0875% Fe, 0.0095% C, 0.0023% H, 0.0015% N) and were 13.0 mm in diameter and 0.89 mm thick with a total geometric surface area (A_g) of 3.00 cm^2. They were degreased in acetone under reflux and chemically etched in an aqueous solution of 17.5% v/v HF (Aldrich, 48 wt % purity, use with extreme caution) and 1% v/v HNO_3 (Caledon, 68−70 wt % purity, use with caution).[17] The "as-received" Ti discs were only degreased and were not chemically etched or electrochemically colored. The automotive clearcoat was Nason SelectClear Fast Flash Clearcoat 496−00 (automobile clearcoat, DuPont Canada, Inc.), which is an acrylic coating cross-linked by a polyisocyanate activator (ratio of 4 parts polymer to 1 part activator); its chemical composition is proprietary. The marine clearcoat was EpoxyKote Clear 72,000 (National Epoxy Coatings), which is an epoxy coating cross-linked by a polyamide activator (ratio of 1 part polymer to 1 part activator); its chemical composition is also proprietary.

Electrochemical Coloring. The electrochemical coloring of all Ti discs was conducted in a temperature-controlled single-compartment Pyrex electrochemical cell with an electrolyte of 7.5 wt.% aqueous NH_4BF_4 (Aldrich, 97+ wt.% purity) maintained at 298 ± 1 K and a large Ti (Johnson-Matthey, 99.7 wt % purity) counter electrode. The coloring employed AC polarization (California Instruments 3 kVA AC Power Source, Model 3001 iM AC power supply) at a fixed V_{AC} with a frequency of f = 60 Hz for coloring time t_{col} = 10 s.[9,10] A distance of ca. 10 cm was maintained between the working and counter electrodes, and the electrolyte was vigorously stirred with a magnetic stirrer. Following coloring, the Ti discs were immediately rinsed with high-purity demineralized water (18.2 MΩ cm, Millipore Milli-Q) and sonicated for t_{son} = 5 min in an ultrasonic bath (Branson 5200, Branson Ultrasonics Corp.) to remove any traces of electrolyte. This procedure ensured excellent reproducibility of the experimental results. The "as-received" and "0 V" (pure Ti) discs refer to discs that were not electrochemically colored. All voltages referred to in this work are AC.

Application of Clearcoats. The polymer clearcoats were applied to the Ti discs utilizing a spin-coater. The clearcoat solutions were applied to the flat face of the discs with a filtered (PTFE membrane filter, Whatman, Inc., 0.45 μm pore size) syringe (1.0 cm^3 luer-slip syringe, National Scientific Co.) in order to cover the entire face. The disk was then spun about its center at a rotational frequency of f = 4000 rpm for spinning time t_s = 20 s leaving a thin, uniform clearcoat layer that was allowed to cure in a dust-free environment. This rotational speed and spinning time created the smoothest films while maintaining a suitable thickness (lower velocities gave a thicker coating that was rippled and higher velocities produced coatings that were too thin).[17]

Vis Reflectance Spectroscopy Measurements. The instrumentation used for the acquisition of vis reflectivity spectra included a high-resolution spectrometer (Ocean Optics, Inc. HR 2000 CG-UV-NIR) capable of detecting in the 200−1100 nm range with a wavelength (λ) resolution of 2 nm and an intensity (I) resolution of 3.2 counts (1 count ≈ 50 photons). It included a 300 μm High-SR fiber optic cable used to transmit the reflected light to the spectrometer. The polished tip of fiber optic cables such as the one employed in this research typically reflects approximately 4% of incoming light. A 100 W incandescent white light bulb (emitting in a λ = 408−1023 nm range) was used as the white light source and was aimed at the disk surface at an angle of 45°. The detecting fiber was aimed at the disk surface at an angle of −45° (a 90° angle with respect to the light source) in order to detect the specularly reflected light. There was no detectable change in the wavelengths of the reflected light with a change in the angle of incidence. The software utilized to collect the data was 00Ibase32TM version 2.0.1.4 (Ocean Optics, Inc.). During the data acquisition, an integration time of t_{int} = 200 ms was employed, along with an average of 50 acquisitions and a boxcar average of 10 data points. The uncertainties associated with reflectance measurements include any loss of information along the fiber-optic cable, as well as the undesired detection of any scattered or diffusely reflected light.

Surface Profilometry Measurements. The surface profiler employed in the clearcoat thickness analysis and surface roughness measurements was a Dektak 8 Stylus Profiler (Veeco Instruments, Inc., vertical resolution of 40 nm, horizontal resolution of 3.43 data points/μm) utilizing a stylus with a tip diameter of 12.5 μm. It should be noted that error may be associated with the representation of surface characteristics (mainly valleys in between peaks) smaller than the tip diameter. The arithmetic surface roughness (R_a) was calculated using eq 1:

$$R_a = \frac{1}{L}\int_{x=0}^{x=L} |y|dx \quad (1)$$

where L is the scan length and y is the vertical deviation of the surface from the mean height. The clearcoat thickness measurements required the removal of the clearcoat from half of the Ti disk prior to scanning the stylus. This was accomplished with acetone (approximately 15 wipes with an acetone-soaked soft lab-wipe) in the case of the acrylic automotive clearcoat and a soft blade (gentle shaving until substrate was reached but not damaged) in the case of the epoxy marine clearcoat. These rather crude approaches were applied in order to minimize any physical damage to the colored layer while effectively removing the clearcoat. As no suitable solvent facilitates local removal of an epoxy clearcoat, the application of a soft blade was the only option that allowed us to cut and remove a section of the protective polymer coating without

Table 1. Rating Criteria for the Adhesion of the Polymer Clearcoats to the Ti Substrates in the Cross-Cut Test

rating	description of failure[a]
5	no peeling or removal
4	trace peeling or removal along incisions or at their intersection
3	jagged removal along incisions up to 1/16 in. (1.6 mm) on either side
2	jagged removal along most of incisions up to 1/8 in. (3.2 mm) on either side
1	removal from most of the area of the "X" under the tape
0	removal beyond the area of the "X"

[a] The description of failure refers to the state of the coating after removal of the tape. A rating of 5 is ideal, with 0 being the worst.

Table 2. Rating Criteria for the Adhesion of the Polymer Clearcoats to the Ti Substrates in the Cross-Hatch Test

rating	description of failure[a]
5	the edges of the cuts are completely smooth; none of the squares of the lattice are detached
4	small flakes of the coating are detached at intersections
3	small flakes of the coating are detached along edges and at intersections of cuts
2	the coating has flaked along the edges and on parts of the squares
1	the coating has flaked along the edges of cuts in large ribbons and whole squares have detached
0	flaking and detachment worse than rating "1"

[a] The description of failure refers to the state of the coating after removal of the tape. A rating of 5 is ideal, with 0 being the worst.

damaging the colored layer. The clearcoat thickness (d_{coat}) was taken as the difference between the average height of the coated surface and the average height of the bare substrate, being careful to exclude irregularities at the substrate/coating boundary created during clearcoat removal.

Contact Angle Measurements. The static contact angle measurements were conducted using a VCA Optima apparatus (AST Products, Inc., resolution of 0.1°) utilizing 1.5 μL sessile droplets of distilled water at 295 ± 1 K. It should be noted that experimental characteristics, such as environmental humidity, can affect the contact angle measurements. As such, experiments were conducted in a humidity-controlled environment.

Adhesion Testing. ASTM adhesion test D3359−02 is a standard method of evaluating the adhesion of coatings in the Canadian automotive industry and consists of two tests: (i) the cross-cut tape test and (ii) the cross-hatch tape test. A different Ti disk was required for each experiment as the technique is destructive. The tests were performed at a certified external laboratory (ACT Laboratories, Inc., 273 Industrial Dr., Hillsdale, MI 49242−1078, USA) that routinely carries out such measurements for the main Canadian automakers. The cross-cut tape test consists of introducing two incisions into the clearcoat layer to form a cross that intrudes down to the metallic substrate. Permacel Brand 99 (ACT #286) tape is then applied over the entire coated face of the disk for 90 s and is subsequently removed. The failure of the coating upon removal of the tape is reported as described in Table 1. The cross-hatch tape test is identical to the cross-cut tape test with the exception that instead of two incisions being made in the form of a cross, numerous incisions in the form of a grid (10 × 10 incisions on each disk) are introduced. The failure of the coating for this test is reported as described in Table 2. The maximum uncertainty in these tests is ±1 rating unit.

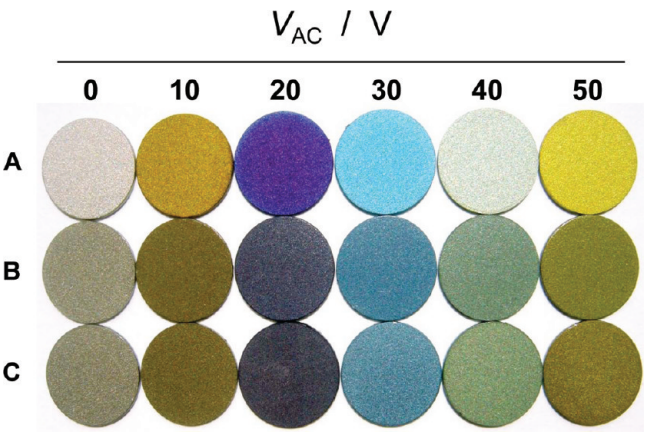

Figure 1. Coloration of passive layers on Ti prepared by the application of AC voltage (V_{AC}) in 7.5 wt % aqueous NH_4BF_4; the polarization time is t_{pol} = 10 s, the AC frequency is f = 60 Hz, and the temperature is T = 298 K. The first column (V_{AC} = 0 V) shows noncolored samples without and with automotive and marine clearcoats. Row A, samples that are colored; row B, samples that are colored and protected with the automotive clearcoat; and row C, samples that are colored and protected with the marine clearcoat. The pictures were taken in outdoor lighting and the backgrounds (the spaces between and around the discs) were digitally removed in order to provide better contrast between the colors.

RESULTS AND DISCUSSION

Electrochemical Coloring and Clearcoat Application. After the native oxide layer was removed from Ti by chemical etching, electrochemical coloring was performed by applying a given V_{AC} in the 10−50 V range for t_{col} = 10 s, with other parameters (electrolyte concentration, temperature, V_{AC} frequency) being constant.[9,10] We present results for varying V_{AC} as it is the variable that is most influential on the colored layer thickness and hence the coloration. Because we used a Ti counter electrode instead of a Pt one as reported in our previous papers, the coloration achieved at a given V_{AC} value slightly differs from that reported elsewhere.[10] We deviated from the earlier procedure because the applicability of a Pt counter electrode in a scaled-up setting is not economically viable. Row A in Figure 1 shows the bright and uniform colored layers prepared by varying V_{AC} between 0 and 50 V (0 V refers to noncolored Ti). We report results for $V_{AC} \leq$ 50 V because the application of higher AC voltages (when using a Ti counter electrode) results in electrical breakdown of the passive layer accompanied by visible and audible sparking that damages the layer (resulting in nonuniform coloration, crack formation and flaking). Once damaged by electrical breakdown, the film loses much of its visual properties and protection against corrosion and weathering. Each color is very reproducible in the sense that it is difficult to visually distinguish between two Ti discs prepared at the same V_{AC}. The coloration originates from thin film constructive light interference (iridescence).[18−21] The rows B and C in Figure 1 present colored passive layers coated in automotive (Row B) and marine (Row C) clearcoats. It can be seen that the clearcoats affect the visual properties of the colored Ti discs only slightly.

Reflectivity in the Vis Region. The manner and extent in which the clearcoats affect the visual properties of the colored layers was investigated through the recording of reflectivity spectra in the vis region of the electromagnetic spectrum. Figure 2

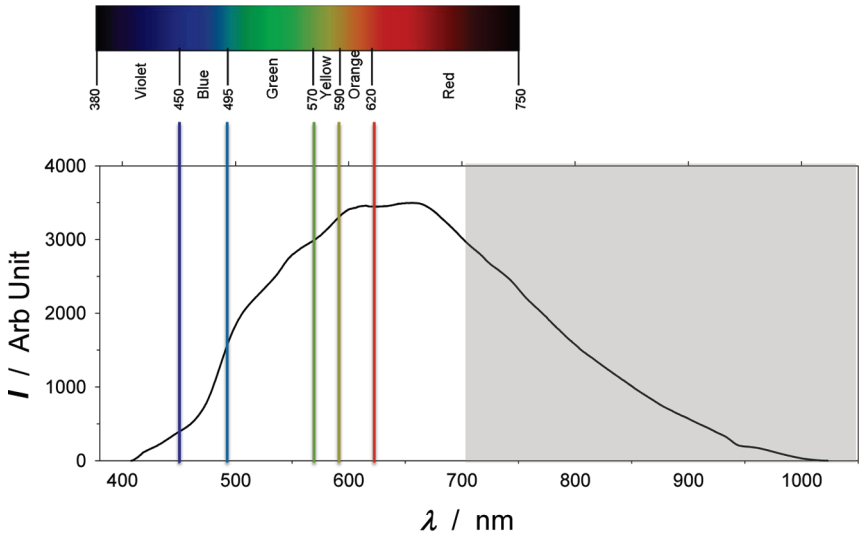

Figure 2. Emission spectrum (I vs λ) of the white light source and assignment chart relating wavelength regions to colors.

presents the emission spectrum (intensity, I, vs wavelength, λ) of the white light source, which also produces near-infrared (NIR) radiation. A vertical dashed line is drawn to separate the vis region (400 nm $\leq \lambda \leq$ 700 nm) from the NIR region (700 nm $\leq \lambda \leq$ 1400 nm). As light in the NIR region does not contribute to the visual characteristics, it is omitted from analysis and discussion. The inset in Figure 2 shows the wavelength assignments for the primary colors of the vis region, and is used to relate the spectra of the colored layers to their exhibited coloration.

Figure 3 presents the reflectivity spectra of each colored layer on Ti, without and with either of the clearcoats. The reflectivity (R) is defined as the fraction of the incident radiation reflected by a surface ($R = I_{refl}/I_{incid}$, where I_{refl} and I_{incid} are the reflected and incident spectral intensities, respectively). The spectra show R in the vis region, which is responsible for the observed coloration. Data for λ < 425 nm have been omitted from the spectra as the signal in this region is weak, making the effects of uncertainty significant.

Figure 3A shows the reflectivity spectra for three samples: (i) etched Ti; (ii) etched Ti with automotive clearcoat; and (iii) etched Ti with marine clearcoat. Figure 3B−F shows the reflectivity spectra for four samples: (i) etched Ti; (ii) etched and colored Ti; (iii) etched and colored Ti with automotive clearcoat; and (iv) etched and colored Ti with marine clearcoat (the V_{AC} values are shown in the Figures). Etched Ti possesses a natural, thin (ca. 2−5 nm) oxide layer that develops upon contact with air; however it is too thin to create any light interference.[22] The spectrum for etched Ti shows that it reflects light over almost the entire vis region, starting at 428 nm and increasing in reflectivity as λ increases.

The reflectivity spectra for the colored but uncoated layers (Figure 3B−F) reveal a significantly reduced value of R over the entire λ range, and relatively small variation of R with λ. The reduction of R translates into reduced brightness upon observation (see Figure 1). Because there are no peaks in the R vs λ plots, the colors exhibited by the passive layers are a combination of all the primary colors in the Vis region. Maxima in the plots indicate color regions that contribute the most to the observed coloration. Conversely, minima indicate color regions that contribute the least. Table 3 lists the wavelengths in the vis region at which R reaches a local maximum value for each passive layer's spectrum (without clearcoat) along with their corresponding colors, hence identifying the components of each passive layer's color.

The spectra of the clearcoat-covered colored layers bear resemblance in shape to those of their uncoated counterparts, however the intensities differ for almost every wavelength in such a manner as to lower the spectral maxima and heighten the spectral minima. This flattening of the reflectivity curves renders the spectra closer to that of white light (a horizontal R vs λ line), causing the colors exhibited by the clearcoated Ti surfaces to be slightly paler shades of the underlying colors. This is the case for all of the colored layers and is well displayed for V_{AC} = 20 and 30 V (see Figures 1 and 3). Unlike the colored surfaces, etched Ti is not iridescent, and instead we see overall reductions in R across the entire spectrum with the shape of the curves remaining the same. It is thought that the application of the clearcoats brings the shapes of the reflectivity curves closer to that of the clearcoats alone.

The change in shape of the reflectivity curves also modifies the overall quantity of vis light reflected by the Ti surfaces (the brightness), which is proportional to the areas under the reflectivity curves. Analysis of the spectra shown in Figure 3 revealed that the area under each curve does not remain constant when a layer of either clearcoat is applied. Whether it increases or decreases depends on the applied V_{AC} during coloration. The area under each spectrum was integrated, and these values are reported in Table 4, which presents the changes to the total reflected vis light that takes place upon clearcoat application. The data are expressed as a percent change with respect to the total vis light reflected by the corresponding uncoated surface. For Ti colored at V_{AC} = 0, 40, and 50 V (the brightest colors) there is a decrease in the total reflected vis light when either clearcoat is applied. The opposite is true for Ti colored at V_{AC} = 20 V (the darkest color). Titanium colored at V_{AC} = 10 and 30 V exhibits colors of an intermediate brightness. Therefore, we conclude that there is no consistent direction to the change that occurs upon clearcoat application. The data also reveal that, in all cases, surfaces coated in marine clearcoat tend to reflect more vis light overall than surfaces coated in automotive clearcoat. This is evident upon visual analysis of the spectra and the data presented

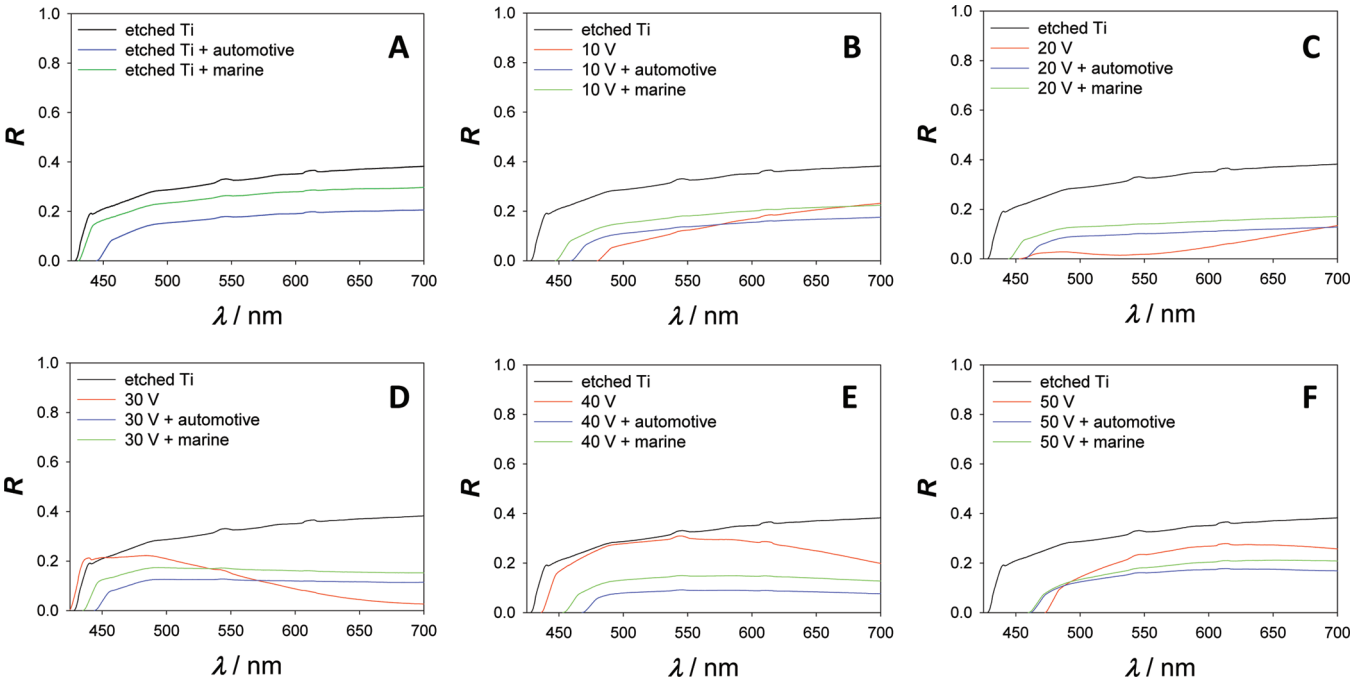

Figure 3. Sets of reflectivity spectra (R vs λ) for: (A) etched Ti without and with clearcoats; (B–F) etched Ti, etched and colored Ti, and etched and colored Ti with clearcoats.

Table 3. Spectral Analysis of the Vis Region of the Reflectivity Spectra for the Ti Passive Layers

	peak(s) in vis region		
V_{AC} (V)	λ (nm)	R (arb unit)	main contributing colors
0 (etched Ti)	700	0.38	all
10	700	0.23	orange, red
20	485/700	0.03/0.13	blue, red
30	483	0.22	blue, green
40	545	0.31	green, yellow
50	613	0.28	yellow, orange

Table 4. Effects of Clearcoat Application on the Total Quantity of Vis Light Reflected by the Ti Surfaces

	% change[a]	
V_{AC} (V)	automotive	marine
0 (etched Ti)	↓ 49	↓ 21
10	0	↑ 34
20	↑ 99	↑ 186
30 V	↓ 16	↑ 18
40 V	↓ 72	↓ 52
50 V	↓ 30	↓ 1

[a] The data are expressed as a percent change with respect to the total visible light reflected by the associated uncoated surface. Arrows refer to an increase or decrease in the total reflected light.

in Table 4. Though the changes in reflectivity shown in Figure 3 and Table 4 are significant (as high as 186%), the visual appearance of the colored layers remains similar to the naked eye (see Figure 1).

Determination of Clearcoat Layer Thicknesses. The thicknesses of the clearcoat layers were determined through measurements with a surface stylus profiler. The clearcoat layer was removed from half of each disk as described in Experimental Section, creating a steplike feature at the half-disk boundary. The stylus was subsequently scanned from the revealed bare substrate, across the feature, to the clearcoat surface, producing topography data from which the clearcoat thickness (d_{coat}) was determined. Figure 4 shows a representative three-dimensional (3D) image of the steplike feature and surrounding region for the 20 V colored layer with marine clearcoat. The image is created from the topographical mapping data collected by the profiler in a 2.0 mm × 2.0 mm sampling area about the substrate-coating boundary. The spikes or peaks at the boundary are local perturbations of the coating created during clearcoat removal, and are excluded from the coating thickness measurements by equating the thickness to the difference between the two average surface heights. It should be mentioned that the vertical features in Figure 4 are shorter in reality than they appear because as the z-direction scale is on the order of micrometers, whereas the x- and y-direction scales are of millimeters. This is necessary in order to render minute surface details visible. The results of the thickness measurements are summarized in Table 5; the values reported are averages of a minimum of 10 acquisitions on a minimum of 3 discs. Upon acquiring each thickness measurement, the arithmetic surface roughness R_a was calculated using eq 1 both for the bare substrate and the coated surface. The sum of these two values was taken as the uncertainty (resulting from surface roughness) of each thickness measurement.

It is evident from the data that the substrate's initial state and coloration (etching, value of V_{AC}) have little effect on the clearcoat layer thickness, as only minor differences are observed

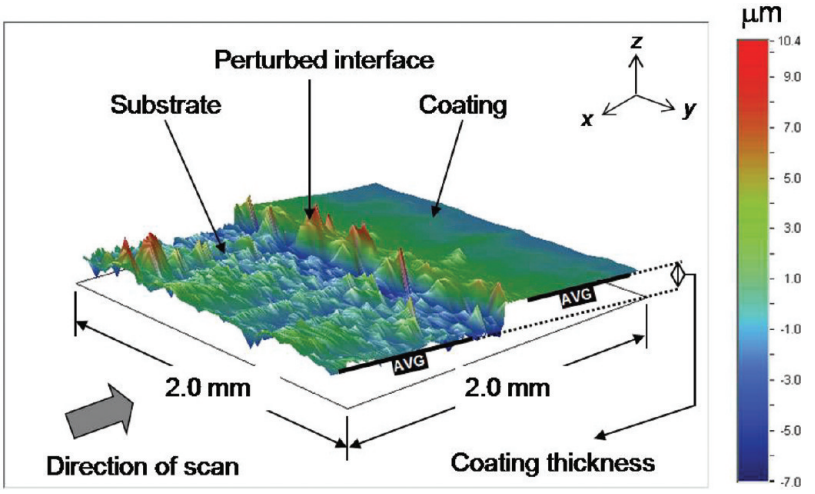

Figure 4. Three-dimensional image of the steplike feature at the edge of the clearcoat for the colored layer formed at V_{AC} = 20 V; the imaging area is 2.0 mm × 2.0 mm.

Table 5. Polymer Layer Thickness Measurements on the Ti Surfaces[a]

	automotive		marine	
V_{AC} (V)	d_{coat} (μm)	R_a (μm)	d_{coat} (μm)	R_a (μm)
as-received Ti	3.31 ± 0.42	0.71	6.93 ± 0.49	0.55
0 (etched Ti)	3.18 ± 0.66	1.06	6.17 ± 0.65	0.74
30	3.00 ± 0.96	1.40	6.10 ± 0.70	0.89
50	3.71 ± 1.18	1.70	6.61 ± 0.55	0.76

[a] Values reported are averages of a minimum of 10 acquisitions on a minimum of 3 discs, and are presented with their standard deviations. The R_a column indicates the uncertainty associated with surface roughness.

Table 6. Arithmetic Surface Roughness, R_a, of Ti without and with the Clearcoats

		R_a[a] (μm)		
sampling area (mm^2)	V_{AC} (V)	uncoated [b]	automotive	marine
6.25	as-received Ti	0.51 ± 0.07	0.34 ± 0.06	0.13 ± 0.04
	0 (etched Ti)	1.30 ± 0.03	0.65 ± 0.07	0.20 ± 0.04
	30	1.50 ± 0.06	0.68 ± 0.07	0.21 ± 0.05
	50	1.58 ± 0.05	0.76 ± 0.09	0.23 ± 0.04
0.16	as-received Ti	0.58 ± 0.18	0.18 ± 0.08	0.05 ± 0.02
	0 (etched Ti)	0.63 ± 0.14	0.35 ± 0.19	0.07 ± 0.04
	30	0.92 ± 0.18	0.41 ± 0.13	0.03 ± 0.01
	50	1.02 ± 0.20	0.56 ± 0.28	0.08 ± 0.04

[a] R_a values reported are averages of at least 60 measurements across a minimum of 3 discs, and are presented with their standard deviations. [b] Values of uncoated Ti for the 6.25 mm^2 sampling area (top four values in "Uncoated" column) were taken from ref.[11]

between the surfaces. The mean thickness of the automotive clearcoat is d_{coat} = 3.3 ± 0.8 μm and that of the marine clearcoat is d_{coat} = 6.5 ± 0.6 μm (twice that of the automotive). Such thicknesses are suitable for application to small items, such as eyeglass frames, watches, cufflinks and other personal items, as the coating offers sufficient protection while avoiding added bulk. Coatings of these thicknesses would also be suitable for decorative applications of Ti (jewelry, ornaments, household items, office supplies, etc.). We have not yet investigated the application of multiple layers of either clearcoat, nor any alternate methods of application, however should either of these prove capable of producing uniform films, and the ability to vary the clearcoat thickness would allow for the tailoring of clearcoat properties (hardness and UV filtration for example) to the object's end-use.

Characterization of Surface Roughness. Previous results from our laboratory have shown that the arithmetic surface roughness (R_a, as defined in Experimental Section) of commercial polycrystalline Ti increases significantly upon etching and upon electrochemical coloring; the roughness increases with increasing V_{AC}.[11] Surface roughness measurements were also performed in this work in order to determine the change in R_a of the Ti surfaces upon application of the clearcoats. As in the previous studies, this was accomplished via surface profilometry measurements, and the results are summarized in Table 6. The R_a values reported are averages of at least 60 measurements across a minimum of 3 discs, and are for sampling areas of 6.25 mm^2 (2.50 mm × 2.50 mm, to examine larger scale roughness) and 0.16 mm^2 (400 μm × 400 μm, to examine small scale roughness). It is expected that "as-received", etched and clearcoat-covered Ti surfaces will possess different morphological characteristics intrinsic to the manufacturing process. For example, the "as-received" Ti samples should show scratches and rather small rolling hills and valleys as they are prepared from an industrial-scale Ti sheet.[11] Chemical etching preferentially dissolves grain boundaries as opposed to grain surfaces, and consequently etched samples are expected to have larger R_a values than "as-received" ones, even though they may appear smoother to the naked eye or upon touch.

Much like Zhao and Jerkiewicz's data for the 6.25 mm^2 sampling area, R_a of uncoated Ti for the 0.16 mm^2 sampling area increases upon etching and with increasing V_{AC}.[11] In the case of the 0.16 mm^2 sampling area, however, the largest increase occurs upon coloring as opposed to upon chemical etching (from V_{AC} = 0 to 30 V, a 46% increase from 0.63 to 0.92 μm). Commercial Ti has a rough grain structure that is revealed upon

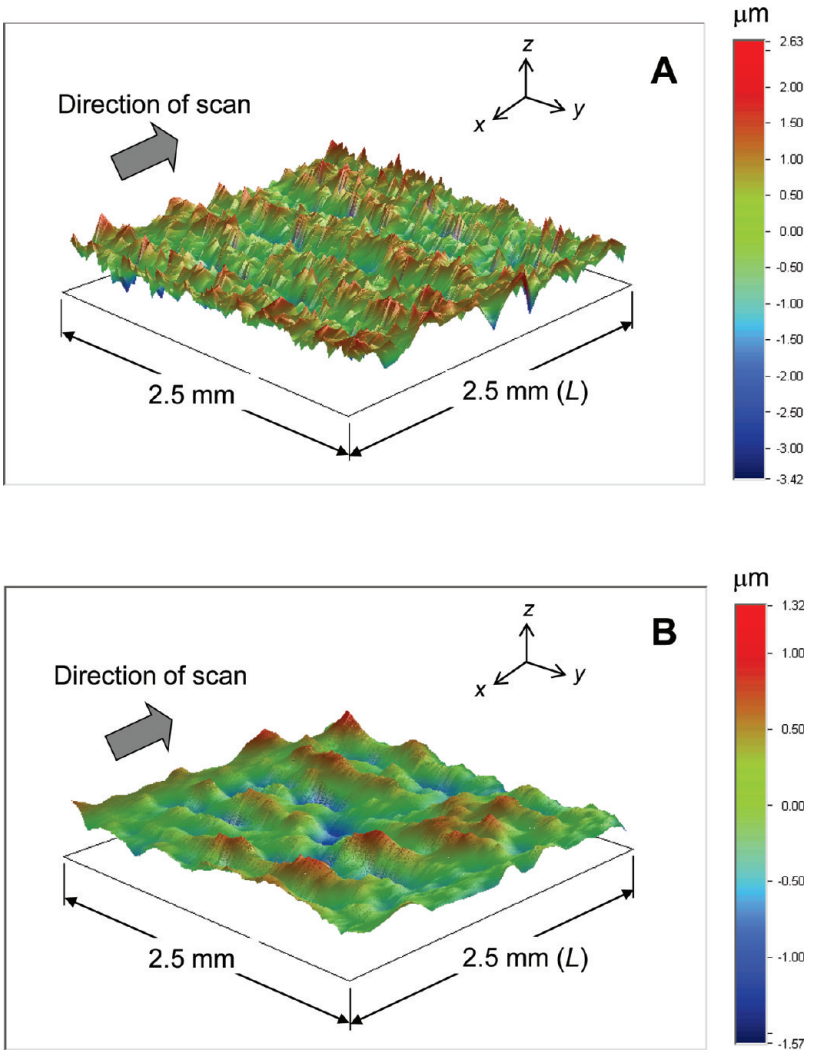

Figure 5. Three-dimensional surface topography segments for the colored layer formed at V_{AC} = 50 V and covered with (A) automotive clearcoat and (B) marine clearcoat; the imaging areas are 2.5 mm × 2.5 mm.

chemical etching for the reasons discussed above, explaining the increase in R_a upon etching. The increases of R_a upon coloring originate from the formation of a thick passive layer through a unique process that involves both the color layer formation and its dissolution; the coloration obtained at a given V_{AC} corresponds to a steady-state thickness.[9−11] With the exception of R_a for the "as-received" surface, which is similar in magnitude when sampling large and small surface areas, R_a of each surface is smaller for the 0.16 mm^2 sampling area than for the 6.25 mm^2 one. This is because the smaller sampling area typically examines one grain at a time, or the connection of two grains, whereas the larger one examines multiple grains at a time and the boundaries in between. In fact, the Ti surfaces are smoother as examined at the 0.16 mm^2 sampling area by 52, 39, and 35% for V_{AC} = 0, 30, 50 V, respectively, when compared to the 6.25 mm^2 sampling area.

The application of both clearcoats was found to reduce the surface roughness of all Ti surfaces significantly for both sampling areas. Upon application of the automotive clearcoat, R_a was reduced by an average of 45 and 53% for the 6.25 and 0.16 mm^2 sampling areas, respectively. In the case of the marine clearcoat, R_a was reduced by an average of 77 and 92%, with reductions as high as 97% (0.16 mm^2, V_{AC} = 30 V). From the data analysis, it is evident that the decrease in R_a is greater upon application of the marine clearcoat than the automotive one. The extent by which the roughness is reduced depends on the roughness of the substrate (related to V_{AC}) and the characteristics of the clearcoat being applied. In the case of the latter, there are two coating properties that dominate the clearcoats' influence on the surface roughness: (i) the inherent roughness of the cured coating finish, which is independent of its substrate and relies on its chemical composition; and (ii) the thickness of the applied layer, as it determines the coating's ability to mask the substrate's topography (i.e., the thicker the layer, the less influence the substrate's roughness has on R_a once coated). In the present case, the automotive and marine clearcoats differ in both of these coating properties, and hence reduce titanium's surface roughness values by different proportions. The marine clearcoat was found not only to cure to a smoother finish but also to produce thicker layers than the automotive clearcoat (6.5 vs 3.3 μm), making it more capable of filling in the intergranular regions of the rough underlying Ti surfaces. It is for these reasons that we see larger decreases in R_a of the Ti surfaces upon application of the marine clearcoat than we do upon application of the automotive one.

Table 7. Static Contact Angles, θ_{stat}, of Water with the Ti Surfaces

	static contact angle, θ_{stat}[a]		
V_{AC} (V)	uncoated[b]	automotive	marine
0 (etched Ti)	67.7 ± 0.5°	92.1 ± 2.4°	83.4 ± 2.4°
30	63.5 ± 0.4°	90.0 ± 1.4°	80.6 ± 2.4°
50	62.4 ± 0.5°	92.8 ± 1.5°	81.9 ± 3.0°

[a] Values reported are averages of at least 10 measurements across a minimum of 3 discs, and are presented with their associated standard deviations. [b] Uncoated values were taken from ref 11.

This is evident when comparing the 3-D images presented in Figure 5, which show 2.5 mm × 2.5 mm surface topography segments for discs colored at V_{AC} = 50 V and coated in each clearcoat (Figure 5A — automotive clearcoat; Figure 5B — marine clearcoat). Again, the vertical features are shorter in reality than they appear as the z-direction scale is on the order of micrometers, whereas the x- and y-direction scales are of millimeters. These reductions in R_a (for both the 6.25 and 0.16 mm^2 sampling areas) are favorable as a smoother surface is beneficial toward reducing wear from friction and the adhesion of fine dirt.

Determination of the Wetting Properties. The wetting properties of Ti are instrumental in its resistance to corrosion and surface weathering. It is preferable, with the exception of physiological applications, to have a surface that wets poorly in order to reduce its deterioration when in humid/aqueous media. The wetting properties of Ti have been shown by Zhao and Jerkiewicz[11] to increase upon electrochemical coloring, as its static contact angle, θ_{stat}, with water decreases with increasing V_{AC}. This is preferable for physiological applications as it is beneficial to have a surface that wets well in order to properly integrate into the body and bond with biological tissues. The opposite is desired for the commercial applications of Ti considered in this contribution, and thus the effects of clearcoat application on θ_{stat} are studied. Poor wetting properties of the clearcoats would reduce the chance of water penetrating the coating surface to locations where it can inflict considerable damage.

The results of the measurements are summarized in Table 7, which reports θ_{stat} obtained with 1.5 μL sessile droplets of distilled water (T = 295 ± 1 K) for the various Ti surfaces. The reported θ_{stat} values are averages of at least 10 measurements across a minimum of 3 discs. The data show that θ_{stat} of all Ti surfaces increases when coated in either of the clearcoats, with surfaces coated in the automotive clearcoat yielding higher θ_{stat} values than those coated in marine one by an average of 10°. The mean increase in θ_{stat} upon coating in automotive clearcoat is 42% with respect to uncoated Ti, and 27% upon coating in marine clearcoat. As all surfaces coated in the same clearcoat have roughly the same θ_{stat} value, regardless of the value of V_{AC} in the case of colored layers, it appears that the substrate's coloration does not directly influence θ_{stat} to a significant extent once coated in clearcoat. As θ_{stat} values increase with clearcoat application, it can be concluded that the wetting properties of the system decrease and that coating in either clearcoat is beneficial toward reducing water exposure to Ti, furthering its protection against corrosion and surface weathering in humid/aqueous environments.

Table 8. Results of ASTM Adhesion Test D3359-02 on Colored Ti Coated in Automotive and Marine Clearcoat

		adhesion rating[a]	
V_{AC} (V)	clearcoat	cross-cut	cross-hatch
as-received Ti	automotive	5	5
	marine	4	2
0 (etched Ti)	automotive	5	5
	marine	5	5
30 V	automotive	5	5
	marine	4	2
60 V	automotive	5	5
	marine	4	3

[a] Rating values defined in Experimental Section.

Characterization of the Adhesion of Clearcoats. Proper adhesion of the clearcoats to the Ti substrates is crucial in their ability to protect the underlying metal. Poor coating adhesion may allow for the formation of voids and blisters at the coating/substrate interface where liquids and gases can accumulate and cause damage.[23] Moreover, a poorly adhered coating will likely chip, exposing segments of the substrate and allowing numerous forms of physical and chemical damage to develop. The adhesion of the clearcoats to the Ti surfaces was examined with the ASTM D3359−02 adhesion tests (cross-cut and cross-hatch tape tests, as defined in the Experimental Section). The results are reported in Table 8. The automotive coating achieved the highest adhesion rating of 5 for all Ti surfaces, both for the cross-cut and cross-hatch tests, indicating that there was no failure of the coating. This rating is what many leading automotive coating manufacturers demand from their coatings and, by their standards, deems the adhesion of the coating to the substrate of adequate strength for use in automotive and possibly other applications. The strong adhesion is thought to be largely attributable to a suitable blend of surfactants in the clearcoat, resulting in good wetting and strong bonding; however, contributions are also made by the clearcoat's low viscosity, which promotes mechanical adhesion. The marine clearcoat did not adhere as well, receiving adhesion ratings in some cases as low as 2, which denotes significant coating flaking and removal during the test. Again, it is thought that the adhesive performance of the clearcoat largely depends on its surfactant content. As such, we conclude that that the marine clearcoat contains a surfactant mix that is tailored in composition and quantity to the steel and aluminum surfaces commonly used in marine environments, and is poorly matched to the relatively polar Ti surfaces (layers of TiO_2, Ti_2O_3).[9,10] Evidence to support this was the visibly poorer wetting of the marine clearcoat to the disk surfaces compared to the ready wetting of the automotive clearcoat. This was noticeable by the higher contact angle upon application of the marine clearcoat and its inability to spread over the entire disk surface, often receding from the edges after application. Another possible contributor is its noticeably higher viscosity, making it more difficult for the coating to spread and mold to the topography of the surfaces, reducing contact and hence both chemical and mechanical adhesion. The marine clearcoat did however adhere well to the etched Ti surface. Discussion of the adhesion of either clearcoat to the Ti surfaces with respect to molecular interactions at the clearcoat/colored layer interface is difficult as the polymer composition of the

clearcoat solutions is proprietary. The only constituent information made public is the identification of the solvents and the activators, along with the fact that the coatings are of the acrylic (automotive) or epoxy (marine) families. With the constituent polymer possibilities being so many, prediction or discussion of the adhesion of the clearcoats in relation to molecular interactions would be mostly speculation and is thus avoided.

CONCLUSIONS

The results have shown that the application of a suitable clearcoat layer to electrochemically colored Ti can significantly protect the colored layers from damage without altering their visual properties in any major way. Protection from chemical damage is provided by significantly decreasing the wetting properties of Ti, resulting in reduced exposure to humid/aqueous media. Protection from physical damage is provided by significantly decreasing the surface roughness, resulting in reduced wear from friction and the adhesion of fine dirt. The thicknesses achieved by spin-coating were of suitable magnitude for small personal applications (eyeglass frames, watches, cufflinks), and would be appropriate for many decorative applications of Ti (jewelry, ornaments, etc.). The automotive clearcoat's adhesion to all Ti surfaces was excellent while the marine clearcoat's was relatively poor. Unlike conventional painting, our reproducible electrochemical coloring and clearcoating procedures create a system that does not rely solely on the polymer coating for its appearance or its protection against corrosion and weathering.

AUTHOR INFORMATION

Corresponding Author

*E-mail: gregory.jerkiewicz@chem.queensu.ca.

ACKNOWLEDGMENT

We gratefully acknowledge financial support from the NSERC of Canada (Discovery Grant, Research Tools and Instruments Grants). A.M. thanks Hans-Peter Loock, Aris Docoslis, Robin Hutchinson, and Baodong Zhao for their helpful advice, as well as Gary Contant for his help in the preparation of the Ti discs.

REFERENCES

(1) Dalard, F.; Montella, C.; Sohm, J. C. *Surf. Technol.* **1976**, *4*, 367.
(2) Dalard, F.; Montella, C.; Gandon, J. *Surf. Technol.* **1979**, *8*, 203.
(3) Ishizawa, H.; Ogino, M. *J. Biomed. Mater. Res.* **1995**, *29*, 65.
(4) Xiong, T.-Y.; Cui, X.-Y.; Kim, H.-M.; Kawashita, M.; Kokubo, T.; Wu, J.; Jin, H.-Z.; Nakamura, T. *Key Eng. Mater.* **2004**, *254*−*256*, 375.
(5) Yang, B.; Uchida, M.; Kim, H.-M.; Zhang, X.; Kokubo, T. *Biomaterials* **2004**, *25*, 1003.
(6) Wong, M. H.; Cheng, F. T.; Man, H. C. *Appl. Surf. Sci.* **2007**, *253*, 7527.
(7) Kuromoto, N. K.; Simão, R. A.; Soares, G. A. *Mater. Charact.* **2007**, *58*, 114.
(8) Lin, C. S.; Chen, M. T.; Liu, J. H. *J. Biomed. Mater. Res. A* **2008**, *85A*, 378.
(9) Jerkiewicz, G.; Strzelecki, H.; Wieckowski, A. *Langmuir* **1996**, *12*, 1005.
(10) Hrapovic, S.; Luan, B. L.; D'Amours, M.; Vatankhah, G.; Jerkiewicz, G. *Langmuir* **2001**, *17*, 3051.
(11) Zhao, B.; Jerkiewicz, G. *Can. J. Chem.* **2006**, *84*, 1132.
(12) Morra, M.; Cassinelli, C. *J. Biomed. Mater. Res.* **1997**, *37*, 198.
(13) Griep-Raming, N.; Karger, M.; Menzel, H. *Langmuir* **2004**, *20*, 11811.
(14) Hayakawa, T.; Yoshinari, M.; Nemoto, K. *Biomaterials* **2004**, *25*, 119.
(15) Munger, C. G. In *Corrosion Prevention by Protective Coatings*; NACE: Houston, 1984.
(16) Hamner, N. E. In *Corrosion Basics: An Introduction*; NACE: Houston, 1984.
(17) Munro, A. J. *Master's Thesis*, Queen's University, Kingston, ON, 2007.
(18) DelPlancke, J.-L.; Degrez, M.; Fontana, A.; Winand, R. *Surf. Technol.* **1982**, *16*, 153.
(19) Gaul, E. *J. Chem. Educ.* **1993**, *70*, 176.
(20) Yau, T.-L. In *Corrosion Engineering Handbook*; Schweitzer, P. A., Ed.; Marcel Dekker: New York, 1996.
(21) Pérez del Pino, A.; Fernández-Pradas, J. M.; Serra, P.; Morenza, J. L. *Surf. Coat. Technol.* **2004**, *187*, 106.
(22) Oliveira, N. T. C.; Biaggio, S. R.; Rocha-Filho, R. C.; Bocchi, N. *J. Biomed. Mater. Res. A* **2005**, *74A*, 397–407.
(23) Schweitzer, P. A. *Corrosion Engineering Handbook*; Marcel Dekker: New York, 1996.